

Article

An Innovative Numerical Method Utilizing Novel Cubic B-Spline Approximations to Solve Burgers' Equation

Ishtiaq Ali ^{1,*} , Muhammad Yaseen ^{2,*} , Muhammad Abdullah ², Sana Khan ²
and Fethi Bin Muhammad Belgacem ³ 

¹ Department of Mathematics and Statistics, College of Science, King Faisal University, P.O. Box 400, Al-Ahsa 31982, Saudi Arabia

² Department of Mathematics, University of Sargodha, Sargodha 40100, Pakistan; muhammadabdullah1831996@gmail.com (M.A.); sanakhanpm28@gmail.com (S.K.)

³ Department of Mathematics, Faculty of Basic Education, Public Authority for Applied Education and Training, Al-Ardhiya 92400, Kuwait; fbmbelgacem@gmail.com

* Correspondence: iamirzada@kfu.edu.sa (I.A.); yaseen.yaqoob@uos.edu.pk (M.Y.)

Abstract: Burgers' equation is a nonlinear partial differential equation that appears in various areas of physics and engineering. Finding accurate and efficient numerical methods to solve this equation is crucial for understanding complex fluid flow phenomena. In this study, we propose a spline-based numerical technique for the numerical solution of Burgers' equation. The space derivative is discretized using cubic B-splines with new approximations for the second order. Typical finite differences are used to estimate the time derivative. Additionally, the scheme undergoes a stability study to ensure minimal error accumulation, and its convergence is investigated. The primary advantage of this scheme is that it generates an approximate solution as a smooth piecewise continuous function, enabling approximation at any point within the domain. The scheme is subjected to a numerical study, and the obtained results are compared to those previously reported in the literature to demonstrate the effectiveness of the proposed approach. Overall, this study aims to contribute to the development of efficient and accurate numerical methods for solving Burgers' equation. The spline-based approach presented herein has the potential to advance our understanding of complex fluid flow phenomena and facilitate more reliable predictions in a range of practical applications.

Keywords: Burgers' equation; cubic B-spline; new cubic B-spline approximation; stability; convergence

MSC: 65M70; 65Z05; 65D05; 65D07; 35B35



Citation: Ali, I.; Yaseen, M.; Abdullah, M.; Khan, S.; Belgacem, F.B.M. An Innovative Numerical Method Utilizing Novel Cubic B-Spline Approximations to Solve Burgers' Equation. *Mathematics* **2023**, *11*, 4079. <https://doi.org/10.3390/math11194079>

Academic Editor: Vladislav Kovalnogov

Received: 26 August 2023

Revised: 21 September 2023

Accepted: 22 September 2023

Published: 26 September 2023



Copyright: © 2023 by the authors. Licensee MDPI, Basel, Switzerland. This article is an open access article distributed under the terms and conditions of the Creative Commons Attribution (CC BY) license (<https://creativecommons.org/licenses/by/4.0/>).

1. Introduction

We consider Burgers' equation (BE) in this study:

$$\frac{\partial v}{\partial t} + v \frac{\partial v}{\partial z} - \lambda \frac{\partial^2 v}{\partial z^2} = 0, \quad z \in [a, b], \quad t > 0, \quad (1)$$

subject to the IC,

$$v(z, 0) = \phi(z) \quad (2)$$

and the BCs,

$$\begin{cases} v(a, t) = \psi_1(t), \\ v(b, t) = \psi_2(t), \end{cases} \quad t > 0, \quad (3)$$

where $\lambda > 0$ and $a, b, \phi(z), \psi_1(t)$ and $\psi_2(t)$ are given.

Burgers' equation was first introduced by Bateman [1] and is a well-known and important model used in various scientific and engineering fields. Fay [2] came up with an interesting series solution for BE, and JM Burgers [3] extensively studied this equation back in 1940, especially in the context of turbulence problems in fluid mechanics. Cole [4] and

Hopf [5] made transformations to turn BE into a linear heat equation, which can be applied with different initial conditions. Additionally, Kreiss and Kreiss [6] delved into the effects of abrupt changes in velocity on how steady-state solutions behave in the Navier–Stokes equation. Miller [7] utilized a predictor-corrector method to model turbulent flow in Burgers' equation. Tian and colleagues [8] presented an intriguing numerical scheme for solving the modified Burgers model with nonlocal dynamic properties. One of the notable features of this work is the use of graded meshes, which are mesh structures that are adaptively refined in regions where the solution exhibits rapid changes or steep gradients. Jiang and his co-authors [9] introduced a predictor-corrector compact difference scheme designed to solve nonlinear fractional differential equations. The proposed scheme addressed the challenges associated with solving nonlinear fractional differential equations efficiently. Rodin [10] discovered several numerical and exact solutions to boundary value problems for BE. Platzman and Benton [11] successfully identified approximately 35 distinct solutions for BE. Graves and Rubin [12] employed quasi-linearization and spline function models to develop numerical techniques for approximating BE. Caldwell et al. [13] introduced a finite element technique for solving BE numerically, and Caldwell and Smith [14] discussed various numerical methods for the computational approximation of BE, generalizing the finite element method for n elements. Kadalbajoo and Awasthi [15] presented a numerical method based on the Crank–Nicolson scheme for solving BE. Rubin and Khosla [16] obtained higher-order numerical solutions of BE using spline and B-spline functions. Caldwell [17] employed cubic splines for the numerical approximation of BE, while [18–20] discussed implicit finite difference schemes based on cubic splines for BE. Ali et al. [21] proposed a B-spline Galerkin technique for numerically approximating BE, and Ali et al. [22] introduced a B-spline collocation method to find the numerical solution to BE. Kutluay et al. [23] investigated BE by using explicit and exact-explicit finite difference methods. Dağ et al. [24,25] presented a numerical solution to BE based on cubic B-spline approximation. Abbasbandy and Darvishi [26] explored the numerical solution of BE using the Adomian decomposition method. Sarboland and Aminataei [27] employed Taylor's meshless Petrov-Galerkin method, utilizing radial basis functions for BE. The choice between B-spline and finite element methods in fluid mechanics applications depends on factors like the complexity of the geometry, desired accuracy, ease of implementation, and specific problem requirements. B-spline methods excel in handling complex geometries and smooth solutions, while finite element methods offer a well-established and versatile approach that is widely adopted in the field. In order to explore further research on Burgers' equation and the related nonlinear phenomenon, please consult [28–38] and the sources cited within.

The primary motivation behind this work is to utilize a novel cubic B-spline approximation for the spatial derivative, leading to an approximate solution of BE with improved accuracy. Another advantage of this approach is that the approximation results in a smooth, piecewise continuous function, enabling approximation at any point within the specified domain.

The rest of the paper is ordered as follows. Section 2 introduces the spline-based numerical technique with a new approximation [39]. In Section 2, the stability of the presented scheme is discussed. Section 4 investigates a convergence analysis of the scheme. Section 5 discusses a comparison of our numerical results with those of some of the other numerical procedures in the literature. Section 6 presents the conclusion of this study.

2. The Derivation of the Scheme

The time and space step sizes are initially defined as $\Delta t = \frac{t}{T}$ and $h = \frac{b-a}{N}$ with T and N being positive integers. Let $t_n = n\Delta t$, $n = 0, 1, 2, \dots, M$, $z_j = jh$, $j = 0, 1, 2, \dots, N$. Now, partition the domain $a \leq z \leq b$ into N equal subintervals $[z_j, z_{j+1}]$, $j = 0, 1, 2, \dots, N - 1$ by

choosing the knots, z_j , where $a = z_0 < z_1 < \dots < z_{n-1} < z_N = b$. The approximation $V(z, t)$ to the exact solution $v(z, t)$ of (1) is given as

$$V(z, t) = \sum_{j=-1}^{N+1} \varepsilon_j(t) B_{3,j}(z), \tag{4}$$

where $\varepsilon_j(t)$ are unknowns to be determined, and the cubic B-Splines (CuBS) basis functions, $B_j^3(z)$, are defined as

$$B_j^3(z) = \frac{1}{6h^3} \begin{cases} (z - z_j)^3, & z \in [z_j, z_{j+1}], \\ h^3 + 3h^2(z - z_{j+1}) + 3h(z - z_{j+1})^2 - 3(z - z_{j+1})^3, & z \in [z_{j+1}, z_{j+2}], \\ h^3 + 3h^2(z_{j+3} - z) + 3h(z_{j+3} - z)^2 - 3(z_{j+3} - z)^3, & z \in [z_{j+2}, z_{j+3}], \\ (z_{j+4} - z)^3, & z \in [z_{j+3}, z_{j+4}], \\ 0, & \text{otherwise.} \end{cases} \tag{5}$$

The local support property of CuBS ensures that only $B_{j-1}^3(z), B_j^3(z)$ and $B_{j+1}^3(z)$ are nonzero at $[z_{j-1}, z_{j+3}], [z_j, z_{j+4}]$, and $[z_{j+1}, z_{j+5}]$, respectively. Consequently, we obtain the approximate solution at the grid point (z_j, t_n) as

$$v(z_j, t_n) = v_j^n = \sum_{k=j-1}^{k=j+1} \varepsilon_k^n(t) B_k^3(z_j). \tag{6}$$

The unknowns $\varepsilon_j^n(t)$ are determined by utilizing the initial, boundary, and collocation conditions applied to $B_j^3(z)$. Through this process, it becomes evident that the approximations v_j^n and their requisite derivatives are given by

$$\begin{cases} v_j^n = \omega_1 \varepsilon_{j-1}^n + \omega_2 \varepsilon_j^n + \omega_1 \varepsilon_{j+1}^n, \\ (v_j^n)_z = -\omega_3 \varepsilon_{j-1}^n + \omega_4 \varepsilon_j^n + \omega_3 \varepsilon_{j+1}^n, \end{cases} \tag{7}$$

where $\omega_1 = \frac{1}{6}, \omega_2 = \frac{4}{6}, \omega_3 = \frac{1}{2h}, \omega_4 = 0$.

The recently derived estimation for the second derivative of $(v_j^n)_{zz}$ is presented in [31] as follows:

$$\begin{cases} (v_0^n)_{zz} = \frac{1}{12h^2} (14\varepsilon_{-1}^n - 33\varepsilon_0^n + 28\varepsilon_1^n - 14\varepsilon_2^n + 6\varepsilon_3^n - \varepsilon_4^n), \\ (v_j^n)_{zz} = \frac{1}{12h^2} (1\varepsilon_{j-2}^n + 8\varepsilon_{j-1}^n - 18\varepsilon_j^n + 8\varepsilon_{j+1}^n + 1\varepsilon_{j+2}^n), \quad j = 1, 2, \dots, N-1 \\ (v_N^n)_{zz} = \frac{1}{12h^2} (-1\varepsilon_{N-4}^n + 6\varepsilon_{N-3}^n - 14\varepsilon_{N-2}^n + 28\varepsilon_{N-1}^n - 33\varepsilon_N^n - 14\varepsilon_{N+1}^n), \end{cases} \tag{8}$$

Equation (1) can be represented in discretized form by discretizing the time derivative by finite differences as

$$\frac{v_j^{n+1} - v_j^n}{\Delta t} + \frac{(vv_z)_j^{n+1} + (vv_z)_j^n}{2} = \lambda \frac{(v_{zz})_j^{n+1} + (v_{zz})_j^n}{2}. \tag{9}$$

Note that the term vv_z is approximated as

$$(vv_z)_j^{n+1} = v_j^n (v_z)_j^{n+1} + v_j^{n+1} (v_z)_j^n - (vv_z)_j^n. \tag{10}$$

so that (9) becomes

$$v_j^{n+1} + \frac{\Delta t}{2} (v_j^n (v_z)_j^{n+1} + v_j^{n+1} (v_z)_j^n) - \frac{\Delta t \lambda}{2} (v_{zz})_j^{n+1} = v_j^n + \frac{\Delta t \lambda}{2} (v_{zz})_j^n. \tag{11}$$

Substituting (7) and (8) in (11) at knot z_0 yields

$$d_1 \varepsilon_{-1}^{n+1} + d_2 \varepsilon_0^{n+1} + d_3 \varepsilon_1^{n+1} + d_4 \varepsilon_2^{n+1} + d_5 \varepsilon_3^{n+1} + d_6 \varepsilon_4^{n+1} = d_7 \varepsilon_{-1}^n + d_8 \varepsilon_0^n + d_9 \varepsilon_1^n - d_4 \varepsilon_2^n - d_5 \varepsilon_3^n - d_6 \varepsilon_4^n, \tag{12}$$

where

$$d_1 = \omega_1 - \frac{7\Delta t \lambda}{12h^2} + \frac{\Delta t(v_z)_0^n \omega_1}{2} - \frac{\Delta t v_0^n \omega_3}{2}, \quad d_2 = \omega_2 + \frac{11\Delta t \lambda}{8h^2} + \frac{\Delta t(v_z)_0^n \omega_2}{2} + \frac{\Delta t v_0^n \omega_4}{2},$$

$$d_3 = \omega_1 - \frac{7\Delta t \lambda}{6h^2} + \frac{\Delta t(v_z)_0^n \omega_1}{2} + \frac{\Delta t v_0^n \omega_3}{2}, \quad d_4 = \frac{7\Delta t \lambda}{12h^2}, \quad d_5 = \frac{-\Delta t \lambda}{4h^2}, \quad d_6 = \frac{\Delta t \lambda}{24h^2},$$

$$d_7 = \omega_1 + \frac{7\Delta t \lambda}{12h^2}, \quad d_8 = \omega_2 - \frac{11\Delta t \lambda}{8h^2}, \quad d_9 = \omega_1 + \frac{7\Delta t \lambda}{6h^2}.$$

By substituting (7) and (8) in (11) at knots z_j , we obtain

$$e_1 \varepsilon_{j-2}^{n+1} + e_2 \varepsilon_{j-1}^{n+1} + e_3 \varepsilon_j^{n+1} + e_4 \varepsilon_{j+1}^{n+1} + e_1 \varepsilon_{j+2}^{n+1} = -e_1 \varepsilon_{j-2}^n + e_5 \varepsilon_{j-1}^n + e_6 \varepsilon_j^n + e_5 \varepsilon_{j+1}^n - e_1 \varepsilon_{j+2}^n, \tag{13}$$

$$j = 1, 2, 3, \dots, N - 1,$$

where

$$e_1 = -\frac{\lambda \Delta t}{24h^2}, \quad e_2 = \omega_1 - \frac{\Delta t \lambda}{3h^2} + \frac{\Delta t(v_z)_j^n \omega_1}{2} - \frac{\Delta t v_j^n \omega_3}{2}, \quad e_3 = \omega_2 + \frac{3\Delta t \lambda}{4h^2} + \frac{\Delta t(v_z)_j^n \omega_2}{2} + \frac{\Delta t v_j^n \omega_4}{2},$$

$$e_4 = \omega_1 - \frac{\Delta t \lambda}{3h^2} + \frac{\Delta t(v_z)_j^n \omega_1}{2} + \frac{\Delta t v_j^n \omega_3}{2}, \quad e_5 = \omega_1 + \frac{\Delta t \lambda}{3h^2}, \quad e_6 = \omega_2 - \frac{3\Delta t \lambda}{4h^2}.$$

Substituting (7) and (8) in (11) at the knot z_N yields

$$g_1 \varepsilon_{N-4}^{n+1} + g_2 \varepsilon_{N-3}^{n+1} + g_3 \varepsilon_{N-2}^{n+1} + g_4 \varepsilon_{N-1}^{n+1} + g_5 \varepsilon_N^{n+1} + g_6 \varepsilon_{N+1}^{n+1} = -g_1 \varepsilon_{N-4}^n - g_2 \varepsilon_{N-3}^n - g_3 \varepsilon_{N-2}^n + g_7 \varepsilon_{N-1}^n + g_8 \varepsilon_N^n + g_9 \varepsilon_{N+1}^n, \tag{14}$$

where

$$g_1 = \frac{\lambda \Delta t}{24h^2}, \quad g_2 = -\frac{\lambda \Delta t}{4h^2}, \quad g_3 = \frac{7\lambda \Delta t}{12h^2}, \quad g_4 = \omega_1 - \frac{7\lambda \Delta t}{6h^2} + \frac{\Delta t(v_z)_N^n \omega_1}{2} - \frac{\Delta t v_N^n \omega_3}{2},$$

$$g_5 = \omega_2 + \frac{11\lambda \Delta t}{8h^2} + \frac{\Delta t(v_z)_N^n \omega_2}{2} + \frac{\Delta t v_N^n \omega_4}{2}, \quad g_6 = \omega_1 - \frac{7\lambda \Delta t}{12h^2} + \frac{\Delta t(v_z)_N^n \omega_1}{2} + \frac{\Delta t v_N^n \omega_3}{2},$$

$$g_7 = \omega_1 + \frac{7\lambda \Delta t}{6h^2}, \quad g_8 = \omega_2 - \frac{11\lambda \Delta t}{8h^2}, \quad g_9 = \omega_1 + \frac{7\lambda \Delta t}{12h^2}.$$

Note that from (12), (13), and (14), a system of $N + 1$ linear equations in $N + 3$ unknowns is obtained. Two additional equations are derived from the stated boundary conditions for a consistent system. As a result, a consistent system of dimensions $(N + 3) \times (N + 3)$ is obtained, which can be uniquely solved using any Gaussian elimination-based numerical approach in a unique manner.

Initial state: The initial vector ε^0 can be obtained from the initial condition and boundary values of the derivatives of the initial conditions as follows:

$$\begin{cases} (v_j^0)_z = \phi'(z_j), & j = 0, \\ (v_j^0) = \phi(z_j), & j = 0, 1, \dots, N, \\ (v_j^0)_z = \phi'(z_j), & j = N. \end{cases} \tag{15}$$

The arrangement (15) results in a matrix system of dimensions $(N + 3) \times (N + 3)$, taking the following structure:

$$A \varepsilon^0 = d, \tag{16}$$

where

$$A = \begin{bmatrix} -\omega_3 & \omega_4 & \omega_3 & 0 & \dots & 0 & 0 \\ \omega_1 & \omega_2 & \omega_1 & 0 & \dots & 0 & 0 \\ 0 & \omega_1 & \omega_2 & \omega_1 & 0 & \dots & 0 \\ \vdots & \vdots & \vdots & \vdots & \vdots & \vdots & \vdots \\ \vdots & \vdots & \vdots & \vdots & \vdots & \vdots & \vdots \\ \vdots & \vdots & \vdots & \vdots & \vdots & \vdots & \vdots \\ 0 & 0 & \dots & \dots & \omega_1 & \omega_2 & \omega_1 \\ 0 & 0 & \dots & \dots & -\omega_3 & \omega_4 & \omega_3 \end{bmatrix},$$

$$\varepsilon^0 = [\varepsilon_{-4}^0, \varepsilon_{-2}^0, \varepsilon_{-1}^0, \dots, \varepsilon_{N-2}^0] \text{ and } d = [\phi'(z_0), \phi(z_0), \dots, \phi(z_N), \phi'(z_N)].$$

3. Stability Analysis

The stability of the suggested method (12)–(14) is demonstrated to be unconditionally stable in this section for the entire domain. Following the von Neumann method, the nonlinear term vv_z is linearized by taking v_z as a constant d . Consequently, the scheme can be linearized as

$$v_j^{n+1} + \frac{\Delta t}{2}dv_j^{n+1} - \frac{\Delta t\lambda}{2}(v_{zz})_j^{n+1} = v_j^n - \frac{\Delta t}{2}dv_j^n + \frac{\Delta t\lambda}{2}(v_{zz})_j^n. \tag{17}$$

By substituting (7) and (8) in (17), we obtain

$$p_0\varepsilon_{j-2}^{n+1} + p_1\varepsilon_{j-1}^{n+1} + p_2\varepsilon_j^{n+1} + p_1\varepsilon_{j+1}^{n+1} + p_0\varepsilon_{j+2}^{n+1} = q_0\varepsilon_{j-2}^n + q_1\varepsilon_{j-1}^n + q_2\varepsilon_j^n + q_1\varepsilon_{j+1}^n + q_0\varepsilon_{j+2}^n, \tag{18}$$

where, $j = 2, 3, 4, \dots, N - 1$ and

$$p_0 = -\frac{\lambda\Delta t}{24h^2}, \quad p_1 = \left(1 + \frac{\Delta td}{2}\right)\omega_1 - \frac{\lambda\Delta t}{3h^2}, \quad p_2 = \left(1 + \frac{\Delta td}{2}\right)\omega_2 + \frac{3\lambda\Delta t}{4h^2},$$

$$q_0 = \frac{\lambda\Delta t}{24h^2}, \quad q_1 = \left(1 - \frac{\Delta td}{2}\right)\omega_1 + \frac{\lambda\Delta t}{3h^2}, \quad q_2 = \left(1 - \frac{\Delta td}{2}\right)\omega_2 - \frac{3\lambda\Delta t}{4h^2}.$$

Now, by inserting the Fourier mode, $\varepsilon_j^n = B\zeta^n \exp(ij\phi h)$ into (18), where B, ζ and ϕ are the harmonics amplitude, growth factor, and the mode number, respectively, and $\iota = \sqrt{-1}$, we obtain

$$p_0B\zeta^{n+1}e^{i(j-2)\phi h} + p_1B\zeta^{n+1}e^{i(j-1)\phi h} + p_2B\zeta^{n+1}e^{ij\phi h} + p_1B\zeta^{n+1}e^{i(j+1)\phi h} + p_0B\zeta^{n+1}e^{i(j+2)\phi h}$$

$$= q_0B\zeta^n e^{i(j-2)\phi h} + q_1B\zeta^n e^{i(j-1)\phi h} + q_2B\zeta^n e^{i(j)\phi h} + q_1B\zeta^n e^{i(j+1)\phi h} + q_0B\zeta^n e^{i(j+2)\phi h}. \tag{19}$$

This implies that

$$B\zeta^n e^{ij\phi h} (p_0\zeta e^{-2i\phi h} + p_1\zeta e^{-i\phi h} + p_2\zeta + p_1\zeta e^{i\phi h} + p_0\zeta e^{2i\phi h})$$

$$= B\zeta^n e^{ij\phi h} (q_0e^{-2i\phi h} + q_1e^{-i\phi h} + q_2 + q_1e^{i\phi h} + q_0e^{2i\phi h}).$$

so that we obtain

$$\zeta = \frac{q_0(e^{-i2\phi h} + e^{i2\phi h}) + q_1(e^{-i\phi h} + e^{i\phi h}) + q_2}{p_0(e^{-i2\phi h} + e^{i2\phi h}) + p_1(e^{-i\phi h} + e^{i\phi h}) + p_2}. \tag{20}$$

By using the identity $\cos(\phi h) = \frac{e^{i\phi h} + e^{-i\phi h}}{2}$ in (20) and simplifying it, we obtain

$$\zeta = \frac{2q_0 \cos 2\phi h + 2q_1 \cos \phi h + q_2}{2p_0 \cos 2\phi h + 2p_1 \cos \phi h + p_2}.$$

Note that $-\pi \leq \varphi \leq \pi$. Without losing generality, choose $\varphi = 0$ so that the last equation reduces to s

$$\zeta = \frac{2q_0 + 2q_1 + q_2}{2p_0 + 2p_1 + p_2} < 1,$$

which confirms the unconditional stability of the proposed scheme.

4. Convergence Analysis

Within this section, we provide an exposition of the convergence analysis for the presented scheme. In order to proceed, it is necessary to refer to the following theorem [29,30].

Theorem 1. *Let $v(z)$ belong to the class of $C^4[a, b]$, and let us consider a partition $a = z_0 < z_1 < \dots < z_{N-1} < z_N = b$ of the interval $[a, b]$. Additionally, let $V^*(z)$ be the unique B-spline function that interpolates the function v and let D^i denote the i^{th} order derivative. Under these conditions, there exist constants σ_i , which are not dependent on the interval size h , satisfying*

$$\|D^i(v - V^*)\|_\infty \leq \sigma_i h^{4-i}, \quad i = 0, 1, 2, 3.$$

Firstly, we start by considering the computed B-spline approximation to Equation (4), which is expressed as follows:

$$V^*(z, t) = \sum_{j=-1}^{N+1} \varepsilon_j^*(t) B_j^3(z).$$

We aim to assess the errors $|v(z, t) - V^*(z, t)|_\infty$ and $|V^*(z, t) - V(z, t)|_\infty$ individually, enabling us to draw inferences about the overall error, $|v(z, t) - V(z, t)|_\infty$. To facilitate this analysis, we introduce alterations to Equation (11) in the subsequent fashion:

$$r^*(z) = v^* + \frac{\Delta t}{2}(vv_z)^* - \frac{\Delta t \lambda}{2}(v_{zz})^*, \tag{21}$$

where, $v^* = v_j^{n+1}$, $(vv_z)^* = v_j^n (v_z)_{j+1}^{n+1} + v_j^{n+1} (v_z)_j^n$, $(v_{zz})^* = (v_{zz})_j^{n+1}$ and $r(z) = v_j^n + \frac{\Delta t \lambda}{2}(v_{zz})_j^n$. Similarly

$$r(z) = v + \frac{\Delta t}{2}(vv_z) - \frac{\Delta t \lambda}{2}(v_{zz}). \tag{22}$$

Equations (12)–(14) can be written in matrix form as

$$M\varepsilon = R, \tag{23}$$

where $R = Ne^n + h$ and

$$M = \begin{bmatrix} \omega_1 & \omega_2 & \omega_1 & 0 & 0 & \dots & \dots & \dots & 0 \\ d_1 & d_2 & d_3 & d_4 & d_5 & d_6 & 0 & \dots & 0 \\ e_1 & e_2 & e_3 & e_4 & e_1 & 0 & 0 & \dots & 0 \\ \vdots & \vdots \\ \vdots & \vdots \\ \vdots & \vdots \\ 0 & \dots & 0 & 0 & e_1 & e_2 & e_3 & e_4 & e_1 \\ 0 & \dots & 0 & g_1 & g_2 & g_3 & g_4 & g_5 & g_6 \\ 0 & \dots & \dots & \dots & 0 & 0 & \omega_1 & \omega_2 & \omega_1 \end{bmatrix}$$

$$N = \begin{bmatrix} 0 & 0 & 0 & 0 & \dots & \dots & \dots & \dots & 0 \\ d_7 & d_8 & d_9 & -d_4 & -d_5 & -d_6 & 0 & \dots & 0 \\ -e_1 & e_5 & e_6 & e_5 & -e_1 & 0 & \dots & \dots & 0 \\ \vdots & \vdots \\ \vdots & \vdots \\ \vdots & \vdots \\ 0 & \dots & \dots & 0 & -e_1 & e_5 & e_6 & e_5 & -e_1 \\ 0 & \dots & 0 & -g_1 & -g_2 & -g_3 & g_7 & g_8 & g_9 \\ 0 & \dots & \dots & \dots & \dots & \dots & 0 & 0 & 0 \end{bmatrix},$$

where $d_1, d_2, d_3, d_4, d_5, d_6, d_7, d_8, d_9, e_1, e_2, e_3, e_4, e_5, e_6, g_1, g_2, g_3, g_4, g_5, g_6, g_7, g_8, g_9$ are given in (12), (13), and (14) and $h = [\psi_1(t_{n+1}), 0, \dots, 0, \psi_2(t_{n+1})]^T, \varepsilon^n = [\varepsilon_{-1}^n, \varepsilon_0^n, \varepsilon_1^n, \dots, \varepsilon_{N+1}^n]^T$.

By substituting v with V in equation (21), the resulting equation can be expressed in matrix form as follows:

$$M\varepsilon^* = R^* \tag{24}$$

By subtracting (24) from (23), we obtain

$$M(\varepsilon^* - \varepsilon) = (R^* - R). \tag{25}$$

Now, by using (21) and (22), we obtain

$$\begin{aligned} |r^*(z_j) - r(z_j)| &= |(v^*(z_j) - v(z_j)) + \frac{\Delta t}{2}(vv_z^*(z_j) - vv_z(z_j)) - \frac{\Delta t\lambda}{2}(v_{zz}^*(z_j) - v_{zz}(z_j))| \\ &\leq |(v^*(z_j) - v(z_j))| + |\frac{\Delta t}{2}(vv_z^*(z_j) - vv_z(z_j))| + |\frac{\Delta t\lambda}{2}(v_{zz}^*(z_j) - v_{zz}(z_j))| \end{aligned} \tag{26}$$

From (26) and theorem (1), we have

$$\begin{aligned} \|R^* - R\| &\leq \sigma_0 h^4 + \|\frac{\Delta t}{2}\| \|v\| \sigma_1 h^3 + \|\frac{\Delta t\lambda}{2}\| \sigma_2 h^2 \\ &= (\sigma_0 h^2 + \|\frac{\Delta t}{2}\| \|v\| \sigma_1 h + \|\frac{\Delta t\lambda}{2}\| \sigma_2) h^2 \\ &= \gamma_1 h^2, \end{aligned} \tag{27}$$

where $\gamma_1 = \sigma_0 h^2 + \|\frac{\Delta t}{2}\| \|v\| \sigma_1 h + \|\frac{\Delta t\lambda}{2}\| \sigma_2$. The matrix M is clearly diagonally dominant and so it is nonsingular, implying that

$$(\varepsilon^* - \varepsilon) = M^{-1}(R^* - R). \tag{28}$$

By utilizing (27), we obtain

$$\|\varepsilon^* - \varepsilon\| \leq \|M^{-1}\| \|R^* - R\| \leq \|M^{-1}\| (\gamma_1 h^2). \tag{29}$$

Let $\mu_{j,i}$ be the elements of the matrix M and $\xi_j, (0 \leq j \leq N + 2)$ be the sum of the matrix M 's j th row; then, we have

$$\xi_0 = \sum_{i=0}^{N+2} \mu_{0,i} = 2\omega_1 + \omega_2,$$

$$\xi_1 = \sum_{i=0}^{N+2} \mu_{1,i} = d_1 + d_2 + d_3 + d_4 + d_5 + d_6,$$

$$\begin{aligned} \zeta_j &= \sum_{i=0}^{N+2} \mu_{j,i} = 2e_1 + e_2 + e_3 + e_4, \quad 2 \leq j \leq N \\ \zeta_{N+1} &= \sum_{i=0}^{N+2} \mu_{N+1,i} = g_1 + g_2 + g_3 + g_4 + g_5 + g_6, \\ \zeta_{N+2} &= \sum_{i=0}^{N+2} \mu_{N+2,i} = 2\omega_1 + \omega_2. \end{aligned}$$

Based on the principles of matrix theory, we have

$$\sum_{j=0}^{N+2} \mu_{g,j}^{-1} \zeta_j = 1, \quad g = 0, 1, \dots, N + 2, \tag{30}$$

where $\mu_{g,j}^{-1}$ are the elements of M^{-1} . Therefore,

$$\|M^{-1}\| = \sum_{j=0}^{N+2} |\mu_{g,j}^{-1}| \leq \frac{1}{\min \zeta_g} = \frac{1}{\tau_l} \leq \frac{1}{|\tau_l|}, \quad 0 \leq g, l \leq N + 2. \tag{31}$$

By substituting (31) into (29), we see that

$$\|e^* - \varepsilon\| \leq \frac{\gamma_1 h^2}{|\tau_l|} = \gamma_2 h^2, \tag{32}$$

where $\gamma_2 = \frac{\gamma_1}{|\tau_l|}$ is constant.

Theorem 2. *The cubic B-splines $\{B_{-1}, B_0, \dots, B_{N+1}\}$ specified in relationship (5) satisfy*

$$\sum_{j=-1}^{N+1} |B_j^3(z)| \leq \frac{5}{3}, \quad 0 \leq z \leq 1.$$

Proof. Consider

$$\begin{aligned} \left| \sum_{j=-1}^{N+1} B_j^3(z) \right| &\leq \sum_{j=-1}^{N+1} |B_j^3(z)| \\ &= |B_{j-1}^3(z)| + |B_j^3(z)| + |B_{j+1}^3(z)| \\ &= \frac{1}{6} + \frac{4}{6} + \frac{1}{6} \\ &= 1. \end{aligned}$$

Now, for $z \in [z_{j+1}, z_{j+2}]$, we have

$$\begin{aligned} |B_{j-2}^3(z)| &\leq \frac{4}{6} \\ |B_{j-1}^3(z)| &\leq \frac{1}{6}, \\ |B_j^3(z)| &\leq \frac{4}{6}, \\ |B_{j+1}^3(z)| &\leq \frac{1}{6}. \end{aligned}$$

Subsequently, we obtain

$$\sum_{j=-1}^{N+1} |B_j^3(z)| = |B_{j-2}^3(z)| + |B_{j-1}^3(z)| + |B_j^3(z)| + |B_{j+1}^3(z)| \leq \frac{5}{3}$$

as required. \square

Now, consider

$$V^*(z) - V(z) = \sum_{j=-1}^{N+1} (\varepsilon_j^* - \varepsilon_j) B_j^3(z). \tag{33}$$

By using Theorem 2 and (32), we produce

$$\begin{aligned} \|V^*(z) - V(z)\| &= \left\| \sum_{j=-1}^{N+1} (\varepsilon_j^* - \varepsilon_j) B_j^3(z) \right\| \\ &\leq \left| \sum_{j=-1}^{N+1} B_j^3(z) \right| \|(\varepsilon_j^* - \varepsilon_j)\| \\ &\leq \frac{5}{3} \gamma_2 h^2. \end{aligned} \tag{34}$$

Theorem 3. Suppose $v(z)$ represents the exact solution, and $V(z)$ is the cubic collocation approximation to $v(z)$. In such a scenario, the proposed approach demonstrates second-order spatial convergence and

$$\|v(z) - V(z)\| \leq \omega h^2, \quad \text{where } \omega = \sigma_0 h^2 + \frac{5}{3} \gamma_2 h^2.$$

Proof. Based on Theorem 1, the following inequality holds:

$$\|v(z) - V^*(z)\| \leq \sigma_0 h^4. \tag{35}$$

By combining Equations (34) and (35), we arrive at

$$\|v(z) - V(z)\| \leq \|v(z) - V^*(z)\| + \|V^*(z) - V(z)\| \leq \sigma_0 h^4 + \frac{5}{3} \gamma_2 h^2 = \omega h^2. \tag{36}$$

where $\omega = \sigma_0 h^2 + \frac{5}{3} \gamma_2$. \square

5. Results and Discussions

This section aims to validate the reliability of the present scheme through various test problems. The accuracy is assessed using two discrete error norms, namely L_2 and L_∞ , which are calculated as follows:

$$L_2 = \|V - V_n\|_2 = h \sum_{j=0}^N |(V(z_j, t_n) - V_j^n)|^2$$

and

$$L_\infty = \|V - V_n\|_\infty = \max_j |V(z_j, t_n) - V_j^n|.$$

The numerical order of convergence (OC) can be ascertained by utilizing the subsequent formula:

$$OC = \frac{\text{Log}(L_\infty(N)/L_\infty(2N))}{\text{Log}(2N/N)}, \tag{37}$$

where $L_\infty(N)$ and $L_\infty(2N)$ denote the errors acquired using a partition count of N and $2N$, correspondingly.

Example 1. Let us consider Equation (1) with boundary conditions:

$$v(0, t) = v(1, t) = 0$$

and the initial condition:

$$v(z, 1) = \frac{z}{1 + \sqrt{\frac{1}{t_0}} \exp(\frac{z^2}{4\lambda})}$$

The exact solution for this problem is given by

$$v(z, t) = \frac{\frac{z}{t}}{1 + \sqrt{\frac{t}{t_0}} \exp(\frac{z^2}{4\lambda t})}$$

where $t_0 = \exp(\frac{1}{8\lambda})$.

The given procedure is employed to solve the aforementioned problem. Figures 1 and 2 display the approximate and exact solutions, showcasing different values of λ at various time instances. Figure 3 presents the 2D and 3D absolute error profiles at $t = 2$. In Table 1, a comparison is made between the numerical solutions obtained in this work and those presented in [24]. Furthermore, Tables 2 and 3 compare the error norms with those reported in [21,22,25]. Table 4 provide the rate of convergence. The approximate solution for Example 1 obtained when $h = 0.05$, $\lambda = 0.01$, $\Delta t = 0.01$, and $t = 2$ is given as

$$V(z, 2) = \begin{cases} z(0.498619 + 0.000425956z - 0.0212431z^2), & z \in [0, \frac{1}{20}) \\ 1.31894 * 10^{-7} + 0.498611z + 0.000584228z^2 - 0.0222983z^3, & z \in [\frac{1}{20}, \frac{1}{10}) \\ 0.0000154133 + 0.498153z + 0.00516864z^2 - 0.0375796z^3, & z \in [\frac{1}{10}, \frac{3}{20}) \\ \vdots & \vdots \\ \vdots & \vdots \\ 8.95319 - 28.4252z + 30.1839z^2 - 10.7175z^3, & z \in [\frac{17}{20}, \frac{9}{10}) \\ 5.10604 - 15.6013z + 15.9352z^2 - 5.44023z^3, & z \in [\frac{9}{10}, \frac{19}{20}) \\ 2.89384 - 8.61542z + 8.58162z^2 - 2.86004z^3, & z \in [\frac{19}{20}, 1). \end{cases}$$

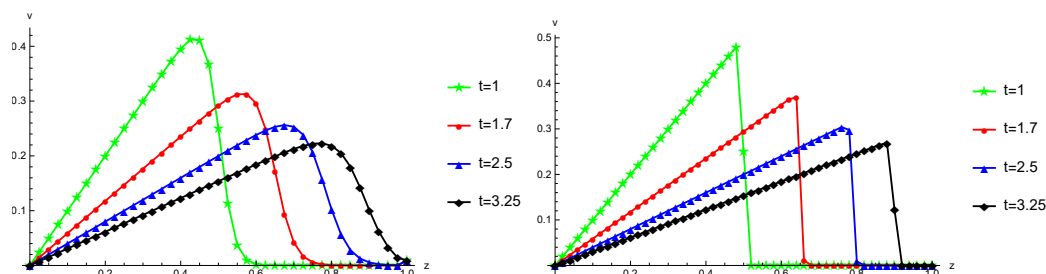


Figure 1. The computed numerical solutions (depicted as diamonds, triangles, circles, and stars) and the exact solutions (illustrated as solid lines) are displayed with a step size of $h = 0.005$, a time increment of $\Delta t = 0.01$, and the parameters $\lambda = 0.005$ (in the left figure) and $\lambda = 0.0005$ (in the right figure) for different time points in Example 1.

Table 1. The computed numerical solutions for Example 1 are shown at various time instances with the parameter $\lambda = 0.0005$, an interval of $[a, b] = [0, 1]$, a step size of $h = 0.005$, and a time increment of $\Delta t = 0.01$.

z	t = 1.7			t = 2.5			t = 3.25		
	CBS [24]	Present	Exact	CBS [24]	Present	Exact	CBS [24]	Present	Exact
0.1	0.05883	0.05882	0.05882	0.04000	0.04000	0.04000	0.03077	0.03077	0.03077
0.2	0.11765	0.11765	0.11766	0.08000	0.08000	0.08000	0.06154	0.06154	0.06154
0.3	0.17648	0.17647	0.17647	0.12001	0.12000	0.12000	0.09231	0.09231	0.09231
0.4	0.23531	0.23529	0.23529	0.16001	0.16000	0.16000	0.12308	0.12308	0.12308
0.5	0.29414	0.29412	0.29412	0.20001	0.20000	0.20000	0.15385	0.15385	0.15385
0.6	0.35296	0.35294	0.35294	0.24001	0.24000	0.24000	0.18462	0.18462	0.18462
0.7	0.00000	0.00000	0.00000	0.28001	0.28000	0.28000	0.21539	0.21538	0.21538
0.8	0.00000	0.00000	0.00000	0.00811	0.00925	0.00976	0.24616	0.24615	0.24615
0.9	0.00000	0.00000	0.00000	0.00000	0.00000	0.00000	0.12358	0.12435	0.12435
CPU time		1.51563			3.23438			4.90625	

Table 2. The error magnitudes for Example 1 were computed with the parameter $\lambda = 0.005$, a step size of $h = 0.005$, and a time increment of $\Delta t = 0.01$ at various time instances.

Ref.	$t = 1.7$		$t = 2.5$		$t = 3.25$	
	L_2	L_∞	L_2	L_∞	L_2	L_∞
[21]	0.857×10^{-3}	2.567×10^{-3}	0.423×10^{-3}	1.242×10^{-3}	0.235×10^{-3}	0.688×10^{-3}
[22]	0.857×10^{-3}	2.567×10^{-3}	0.423×10^{-3}	1.242×10^{-3}	0.235×10^{-3}	0.668×10^{-3}
QBCM [25]	0.07215×10^{-3}	0.31153×10^{-3}	0.05103×10^{-3}	0.18902×10^{-3}	1.24901×10^{-3}	8.98390×10^{-3}
CBCM [25]	2.46642×10^{-3}	27.5770×10^{-3}	2.11187×10^{-3}	25.1517×10^{-3}	1.92482×10^{-3}	21.0489×10^{-3}
Present	1.5719×10^{-5}	5.7239×10^{-5}	1.61443×10^{-5}	1.15023×10^{-4}	1.1067×10^{-3}	7.99793×10^{-3}
CPU time	1.59375	1.59375	3.26563	3.26563	5.03125	5.03125

Table 3. The error magnitudes for Example 1 were calculated for different time points using the parameter $\lambda = 0.0005$, a step size of $h = 0.005$, and a time increment of $\Delta t = 0.01$.

Ref.	$t = 1.7$		$t = 2.5$		$t = 3.25$	
	L_2	L_∞	L_2	L_∞	L_2	L_∞
[21]	0.235×10^{-3}	0.688×10^{-3}	0.567×10^{-3}	5.880×10^{-3}	0.308×10^{-3}	2.707×10^{-3}
[22]	0.567×10^{-3}	5.880×10^{-3}	0.308×10^{-3}	2.705×10^{-3}	0.239×10^{-3}	2.291×10^{-3}
QBCM [25]	1.24624×10^{-3}	13.8155×10^{-3}	1.43951×10^{-3}	16.7712×10^{-3}	1.24624×10^{-3}	13.8155×10^{-3}
CBCM [25]	2.46642×10^{-3}	27.5770×10^{-3}	2.11186×10^{-3}	25.1517×10^{-3}	1.92482×10^{-3}	21.0489×10^{-3}
Present	1.10433×10^{-3}	13.4180×10^{-3}	3.88500×10^{-4}	3.34548×10^{-3}	2.01052×10^{-4}	1.60369×10^{-3}
CPU time	1.51563	1.51563	3.23438	3.23438	4.90625	4.90625

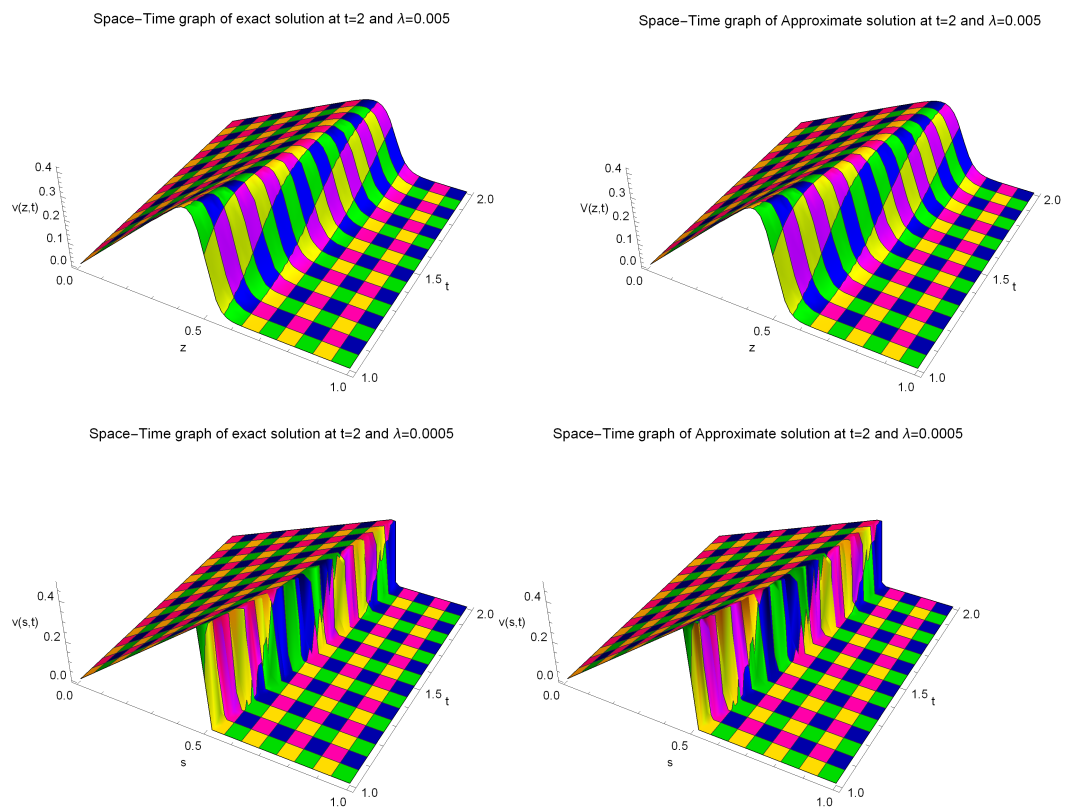


Figure 2. The solutions obtained through numerical computation and the exact solutions for Example 1 are presented while considering the parameter values: $h = 0.005$ and $\Delta t = 0.01$, along with two different values for λ , namely $\lambda = 0.005$ and $\lambda = 0.0005$.

Table 4. The convergence rate assessment was conducted for various values of N in Example 1 by considering the following parameters: $\Delta t = 0.01$, $\lambda = 0.005$, and $t = 2$.

N	L_∞	Ratio	Order of Convergence	CPU Time
25	1.59993×10^{-3}	–	–	0.171875
50	9.98107×10^{-5}	16.0296	4.00267	0.34375
100	4.16944×10^{-5}	2.39386	1.25934	0.890625
200	4.09150×10^{-5}	1.01905	0.02723	2.26563
400	4.09666×10^{-5}	0.99874	0.01821	8.28125

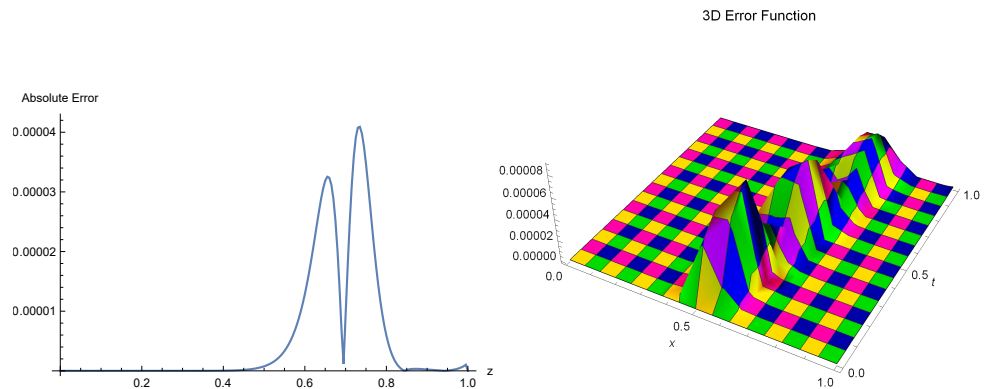


Figure 3. The error distributions in both two-dimensional (2D) and three-dimensional (3D) settings at time $t = 2$ are displayed for Example 1, where the step size is set to $h = 0.005$ and the time increment is $\Delta t = 0.01$.

Example 2. Let us examine equation (1) with the subsequent boundary conditions:

$$v(0, t) = 1, \dots, v(1, t) = 0.2.$$

The precise solution for this scenario is expressed as $v(z, t) = \frac{\mu + \alpha + (\alpha - \mu)e^{\eta}}{1 + e^{\eta}}$, where α , μ , and γ denote arbitrary constants, and $\eta = \frac{\alpha(z - \mu t - \gamma)}{\lambda}$. The initial condition corresponds to $t = 0$ in the exact solution.

Figure 4 depicts the implementation of the presented scheme, as well as approximations to the exact solution at various times. The approximate and exact solutions are depicted in superb 3D contrast in Figure 5. The 2D and 3D error graphs are displayed in Figure 6. Table 5 compares the obtained numerical solutions with the ones reported in [22,37]. The approximate solutions in Table 6 are compared to those found in [20,24,28]. The convergence rate assessment is given in Table 7.

The estimated solution for Example 2 under the conditions of $h = 0.05$, $\lambda = 0.01$, $\Delta t = 0.01$, and $t = 1$ is given by

$$V(z, 1) = \begin{cases} 1. + 0.637846z - 22.0811z^2 + 186.572z^3, & z \in [0, \frac{1}{20}) \\ 1.02956 - 1.13559z + 13.3875z^2 - 49.8856z^3, & z \in [\frac{1}{20}, \frac{1}{10}) \\ 0.966145 + 0.766774z - 5.6361z^2 + 13.5264z^3, & z \in [\frac{1}{10}, \frac{3}{20}) \\ \vdots & \vdots \\ \vdots & \vdots \\ 7.70131 - 24.513z + 26.7269z^2 - 9.72239z^3, & z \in [\frac{17}{20}, \frac{9}{10}) \\ 2.69213 - 7.81572z + 8.17434z^2 - 2.85108z^3, & z \in [\frac{9}{10}, \frac{19}{20}) \\ 0.44573 - 0.721823z + 0.707083z^2 - 0.23099z^3, & z \in [\frac{19}{20}, 1). \end{cases}$$

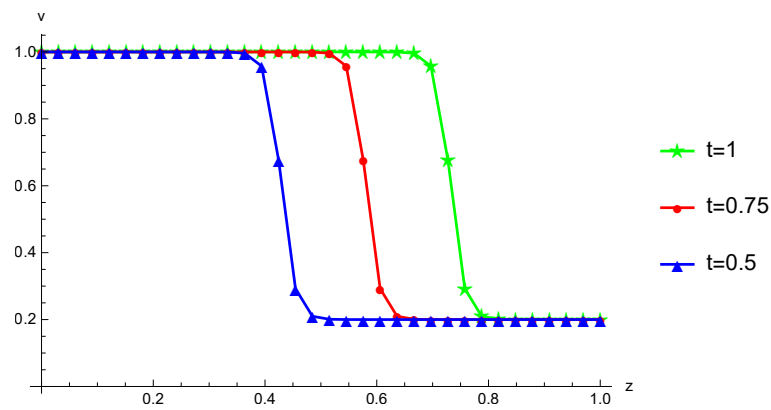


Figure 4. The computed approximate solutions (depicted as triangles, circles, and stars) and the corresponding exact solutions (illustrated as solid lines) for Example 2 are displayed across various time instances, considering the following parameter values: $h = 0.005$, $\Delta t = 0.01$, and $\lambda = 0.005$.

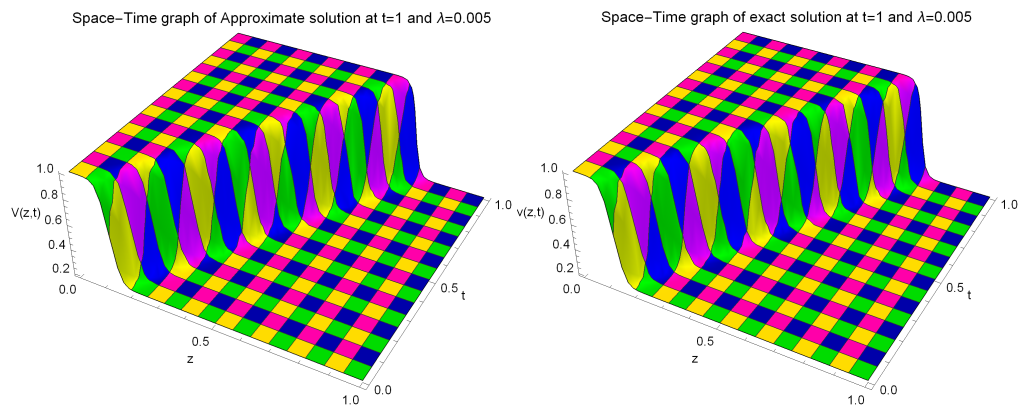


Figure 5. The estimated solution (depicted on the left) and the precise solution (displayed on the right) are presented with the following parameter values: $\lambda = 0.005$, $h = 0.005$, $\Delta t = 0.01$, and $t = 1$ for Example 2.

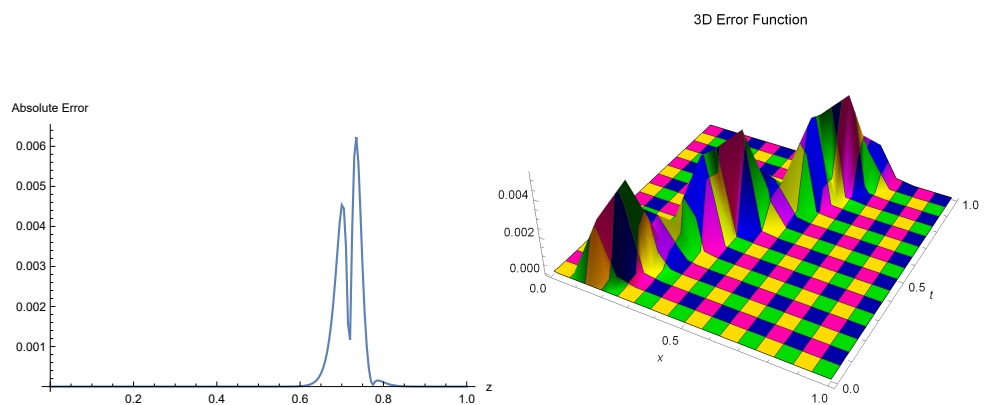


Figure 6. The error distributions in both two-dimensional (2D) and three-dimensional (3D) contexts for Example 2 are shown, employing the parameters $h = 0.005$ and $\Delta t = 0.01$.

Table 5. The computed numerical solutions for Example 2 are obtained with the given parameter values: $h = 0.01$, $\Delta t = 0.001$, and $\lambda = 0.01$.

$t = 0.5$					$t = 1.3$				
z	Present	[37]	[22]	Exact	z	Present	[37]	[22]	Exact
0.3082	0.9928	0.9943	0.9953	0.9926	0.7841	0.9937	0.9974	0.9942	0.9937
0.3542	0.9563	0.9570	0.9609	0.9555	0.8339	0.9564	0.9613	0.9575	0.9560
0.3809	0.8844	0.8849	0.8844	0.8830	0.8618	0.8804	0.8885	0.8812	0.8793
0.4030	0.7673	0.7699	0.7670	0.7655	0.8844	0.7559	0.7703	0.7576	0.7561
0.4456	0.4453	0.4484	0.4446	0.4439	0.9245	0.4521	0.4645	0.4512	0.4515
0.4632	0.3435	0.3484	0.3451	0.3426	0.9371	0.3746	0.3850	0.3757	0.3735
0.4824	0.2735	0.2788	0.2742	0.2732	0.9495	0.3156	0.3244	0.3134	0.3154
0.5076	0.2284	0.2331	0.2279	0.2283	0.9631	0.2701	0.2779	0.2779	0.2713
0.5520	0.2049	0.2087	0.2044	0.2049	0.9791	0.2346	0.2431	0.2463	0.2393
CPU time	4.8125					12.078			

Table 6. The computed numerical solutions for Example 2 were derived by considering the following parameters: $\lambda = 0.01$, time $t = 0.5$, and interval $[a, b] = [0, 1]$.

z	Present	Present	CBS [24]	CBS [24]	PGM [20]	PY [20]	CD [20]	QBGT [28]	Exact
	$h = \frac{1}{36}$ $\Delta t = 0.025$	$h = \frac{1}{18}$ $\Delta t = 0.001$	$h = \frac{1}{36}$ $\Delta t = 0.025$	$h = \frac{1}{18}$ $\Delta t = 0.001$	$h = \frac{1}{36}$ $\Delta t = 0.025$				
0.056	1.000	1.000	1.000	1.000	1.000	1.000	1.030	1.000	1.000
0.111	1.000	1.000	1.000	1.000	1.000	1.000	0.990	1.000	1.000
0.167	1.000	0.999	1.000	1.000	0.998	0.999	1.009	1.000	1.000
0.278	0.999	0.995	0.999	0.996	0.911	0.997	1.004	0.999	0.998
0.333	0.983	0.985	0.986	0.994	0.970	0.982	0.986	0.985	0.980
0.389	0.852	0.845	0.850	0.835	0.862	0.850	0.696	0.847	0.847
0.444	0.449	0.449	0.448	0.461	0.461	0.444	0.360	0.452	0.452
0.500	0.238	0.238	0.236	0.240	0.159	0.171	0.228	0.238	0.238
0.556	0.204	0.204	0.204	0.199	0.300	0.286	0.203	0.204	0.204
0.611	0.200	0.200	0.200	0.199	0.194	0.197	0.200	0.200	0.200
0.667	0.200	0.200	0.200	0.200	0.213	0.211	0.200	0.200	0.200
0.722	0.200	0.200	0.200	0.200	0.211	0.210	0.200	0.200	0.200
0.778	0.200	0.200	0.200	0.200	0.188	0.190	0.200	0.200	0.200
0.833	0.200	0.200	0.200	0.200	0.201	0.207	0.200	0.200	0.200
0.889	0.200	0.200	0.200	0.200	0.191	0.193	0.200	0.200	0.200
0.944	0.200	0.200	0.200	0.200	0.203	0.202	0.200	0.200	0.200
CPU time	0.063	0.672							

Table 7. The convergence rate assessment for Example 2 was conducted at time $t = 1$, considering the various values of N while maintaining $\Delta t = 0.01$.

N	L_∞	Ratio	Order of Convergence	CPU Time
16	2.70279×10^{-2}	–	–	0.10938
32	4.50510×10^{-3}	5.99940	2.58482	0.21875
64	2.33022×10^{-3}	1.93334	0.95109	0.56250
128	2.26236×10^{-3}	1.02999	0.04264	1.26563
256	2.26042×10^{-3}	1.00086	0.00124	4.79688

Example 3. Let us consider Equation (1) with the initial condition

$$v(z, 0) = \text{Sin}(\pi z)$$

and the boundary conditions

$$v(0, t) = 0, v(1, t) = 0.$$

The exact solution for this problem is given by

$$v(z, t) = \frac{4\pi\lambda \sum I_j(\frac{1}{2\pi\lambda}) \text{Sin}(j\pi z) \exp(-j^2\pi^2\lambda t)}{I_0(\frac{1}{2\pi\lambda}) + 2 \sum I_j(\frac{1}{2\pi\lambda}) \text{Cos}(j\pi z) \exp(-j^2\pi^2\lambda t)}$$

Here, I_j represents the modified Bessel function of the first kind.

We employ the current scheme to obtain approximate solutions to this problem. Figure 7 presents the numerical and exact solutions at various time instances. A 3D comparison between the numerical and exact solutions is depicted in Figure 8. Furthermore, Tables 8 and 9 provide evidence of the superiority of our approach by comparing the numerical solutions with those presented in [24].

The computed approximate solution for Example 3, which was obtained by using the following parameter values: $h = 0.05$, $\lambda = 1$, $\Delta t = 0.01$, and $t = 1$, is given by

$$V(z, 1) = \begin{cases} -1.69407 \times 10^{-21} + 0.000170474z - 0.000339192z^2 + 0.00260343z^3, & z \in [0, \frac{1}{20}) \\ 4.53619 \times 10^{-7} + 0.000143257z + 0.000205151z^2 - 0.00102553z^3, & z \in [\frac{1}{20}, \frac{1}{10}) \\ -5.33322 \times 10^{-7} + 0.000172865z - 0.0000909316z^2 - 0.0000385855z^3, & z \in [\frac{1}{10}, \frac{3}{20}) \\ \vdots \\ \vdots \\ 0.0000428039 + 0.00012479z - 0.000206725z^2 + 0.0000385973z^3, & z \in [\frac{17}{20}, \frac{9}{10}) \\ -0.000676679 + 0.00252307z - 0.00287148z^2 + 0.00102554z^3, & z \in [\frac{9}{10}, \frac{19}{20}) \\ 0.00243469 - 0.00730232z + 0.00747104z^2 - 0.00260341z^3, & z \in [\frac{19}{20}, 1). \end{cases}$$

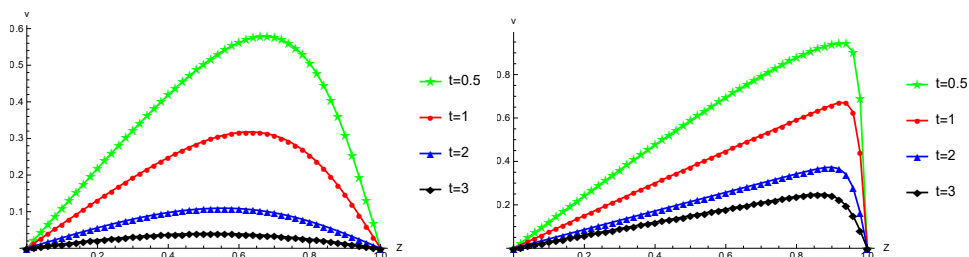


Figure 7. The computed numerical solutions (indicated by triangles, circles, and stars) and the corresponding exact solutions (shown as solid lines) are presented for Example 3. These are displayed for two cases: one with $h = 0.01 = \Delta t$ and $\lambda = 0.1$ (in the left figure), and another with $\lambda = 0.01$ (in the right figure), across various time points.

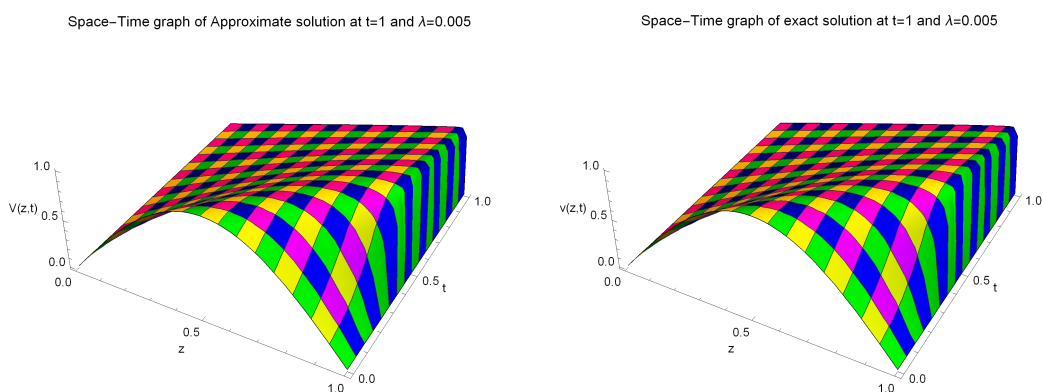


Figure 8. The estimated solution (on the left) and the precise solution (on the right) for Example 3 are presented with parameter values of $h = 0.005$, $\Delta t = 0.01$, and $t = 1$.

Example 4. Let us examine equation 1 with the provided initial condition:

$$v(z, 0) = z$$

and the following boundary conditions

$$v(0, t) = 0, v(1, t) = \frac{1}{1 + t}.$$

The precise solution for this scenario is expressed as

$$v(z, t) = \frac{z}{1 + t}.$$

Table 8. A contrast of the solutions at different positions was performed for Example 3 at time $t = 0.1$, utilizing parameters $\lambda = 1$ and $\Delta t = 0.00001$.

z	h = 0.1		h = 0.05		h = 0.025		h = 0.0125		h = 0.00625		Exact
	CBS [24]	Present	CBS [24]	Present	CBS [24]	Present	CBS [24]	Present	CBS [24]	Present	
0.1	0.10888	0.10954	0.10937	0.10954	0.10949	0.10954	0.10952	0.10954	0.10953	0.10954	0.10954
0.2	0.20847	0.20979	0.20945	0.20979	0.20969	0.20979	0.20975	0.20979	0.20977	0.20979	0.20979
0.3	0.28992	0.29190	0.29138	0.29190	0.29175	0.29190	0.29184	0.29190	0.29186	0.29190	0.29190
0.4	0.34537	0.34792	0.34726	0.34792	0.34773	0.34792	0.34785	0.34792	0.34788	0.34792	0.34792
0.5	0.36859	0.37157	0.37080	0.37158	0.37136	0.37158	0.37149	0.37158	0.37153	0.37158	0.37158
0.6	0.35589	0.35904	0.35823	0.35905	0.35881	0.35905	0.35896	0.35905	0.35900	0.35905	0.35905
0.7	0.30696	0.30989	0.30914	0.30990	0.30969	0.30991	0.30983	0.30991	0.30986	0.30991	0.30991
0.8	0.22552	0.22781	0.22722	0.22782	0.22765	0.22782	0.22776	0.22782	0.22778	0.22782	0.22782
0.9	0.11942	0.12068	0.12036	0.12069	0.12060	0.12069	0.12065	0.12069	0.12067	0.12069	0.12069
CPU time		09.9242		21.4764		39.2374		103.675		237.885	

Table 9. The estimated solutions for Example 3 were computed by using a step size of $h = 0.0125$ and a time increment of $\Delta t = 0.0001$, considering various values of λ .

z	t	$\lambda = 1$			$\lambda = 0.1$			$\lambda = 0.01$			CPU
		CBS [24]	Present	Exact	CBS [24]	Present	Exact	CBS [24]	Present	Exact	
0.25	0.4	0.01357	0.01357	0.01357	0.30890	0.30889	0.30889	0.34192	0.34191	0.34191	43.7382
	0.6	0.00189	0.00189	0.00189	0.24075	0.24074	0.24074	0.26897	0.26896	0.26896	62.5638
	0.8	0.00026	0.00026	0.00026	0.19569	0.19568	0.19568	0.22148	0.22148	0.22148	84.5875
	1.0	0.00004	0.00004	0.00004	0.16258	0.16256	0.16256	0.18819	0.18819	0.18819	143.657
	3.0	0.00000	0.00000	0.00000	0.02720	0.02720	0.02720	0.07511	0.07511	0.07511	332.875
0.50	0.4	0.01923	0.01924	0.01924	0.56965	0.56963	0.56963	0.66071	0.66071	0.66071	43.7382
	0.6	0.00267	0.00267	0.00267	0.44723	0.44721	0.44721	0.52942	0.52942	0.52942	62.5638
	0.8	0.00037	0.00037	0.00037	0.35925	0.35924	0.35924	0.43914	0.43914	0.43914	84.5875
	1.0	0.00005	0.00005	0.00005	0.29192	0.29192	0.29192	0.37442	0.37442	0.37442	143.657
	3.0	0.00000	0.00000	0.00000	0.04019	0.04021	0.04021	0.15018	0.15018	0.15018	332.875
0.75	0.4	0.01362	0.01363	0.01363	0.62538	0.62544	0.62544	0.91027	0.91026	0.91026	43.7382
	0.6	0.00189	0.00189	0.00189	0.48715	0.48721	0.48721	0.76725	0.76724	0.76724	62.5638
	0.8	0.00026	0.00026	0.00026	0.37385	0.37392	0.37392	0.64740	0.64740	0.64740	84.5875
	1.0	0.00004	0.00004	0.00004	0.28741	0.28747	0.28747	0.55605	0.55605	0.55605	143.657
	3.0	0.00000	0.00000	0.00000	0.02976	0.02977	0.02977	0.22483	0.22481	0.22481	332.875

By utilizing the current method, numerical outcomes are acquired for this particular problem. The exact and computed solutions are exhibited at different time instances in Figure 9. A three-dimensional comparison between the precise and estimated solutions at $t = 1$ is depicted in Figure 10. Furthermore, Figure 11 visualizes the two-dimensional and three-dimensional error profiles at $t = 1$. In Table 10, a comparison of error norms is presented, which is in line with the findings reported in [39]. The estimated solution for Example 4 with parameters $h = 0.05$, $\lambda = 0.01$, $\Delta t = 0.01$, and $t = 1$ is as follows:

$$V(z, 1) = \begin{cases} 8.67362 \times 10^{-19} + 0.5z - 2.03393 \times 10^{-13}z^2 + 1.4353 \times 10^{-12}z^3, & z \in [0, \frac{1}{20}) \\ 4.68375 \times 10^{-17} + 0.5z - 1.49214 \times 10^{-13}z^2 + 1.06581 \times 10^{-12}z^3, & z \in [\frac{1}{20}, \frac{1}{10}) \\ 7.00828 \times 10^{-15} + 0.5z + 1.9682 \times 10^{-12}z^2 - 5.92593 \times 10^{-12}z^3, & z \in [\frac{1}{10}, \frac{3}{20}) \\ \vdots \\ \vdots \\ -0.00146154 + 0.505101z - 0.00593043z^2 + 0.0022971z^3, & z \in [\frac{17}{20}, \frac{9}{10}) \\ 0.00645988 + 0.478696z + 0.0234082z^2 - 0.00856906z^3, & z \in [\frac{9}{10}, \frac{19}{20}) \\ -0.0282991 + 0.588461z - 0.0921341z^2 + 0.0319721z^3, & z \in [\frac{19}{20}, 1). \end{cases}$$

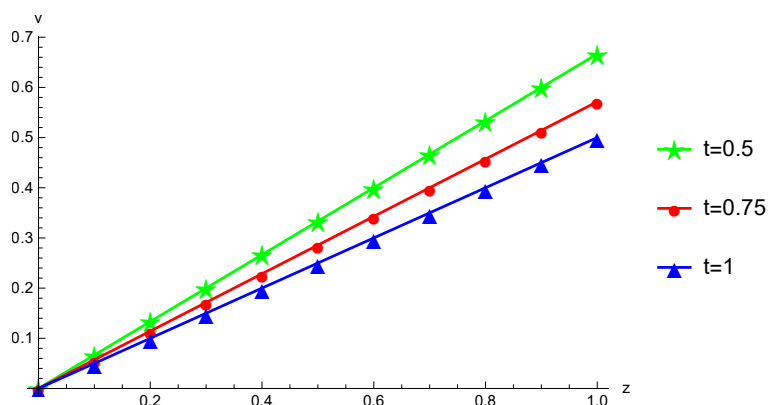


Figure 9. The computed numerical solutions (indicated by triangles, circles, and stars) and the corresponding exact solutions (depicted as solid lines) for Example 4 are presented across various time points, considering the following parameters: $h = 0.01 = \Delta t$ and $\lambda = 1$.

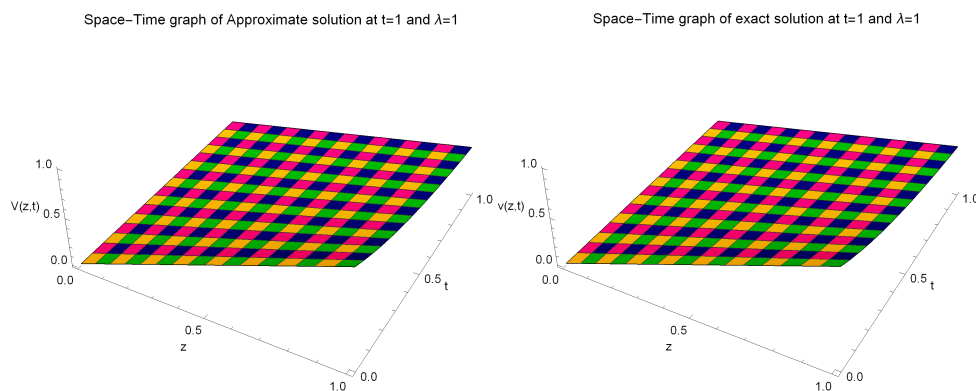


Figure 10. The estimated solution (on the left) and the accurate solution (on the right) for Example 4 are presented with parameter values of $h = 0.01$, $\Delta t = 0.01$, and $t = 1$.

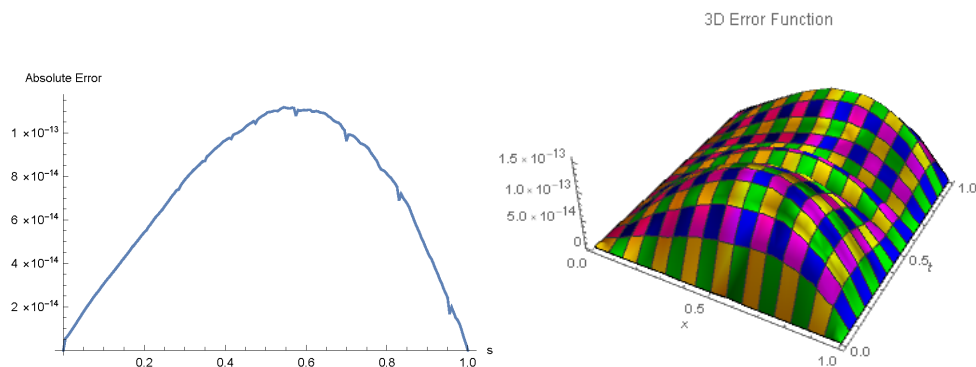


Figure 11. The error distributions in both two-dimensional (2D) and three-dimensional (3D) contexts for Example 4 are displayed under the conditions of $h = 0.01$, $\Delta t = 0.01$, and $\lambda = 1$.

Table 10. Error magnitudes for Example 4 at time $t = 1$ are evaluated across various values of N while maintaining $\Delta t = 0.01$.

N	CuTBS [39]		Present Scheme			
	L_2	L_∞	L_2	L_∞	OC	CPU
10	1.0998×10^{-5}	1.5328×10^{-5}	1.31437×10^{-16}	3.33067×10^{-16}	–	0.07813
20	2.7422×10^{-6}	3.8217×10^{-6}	8.03739×10^{-16}	1.33227×10^{-15}	2.00000	0.14063
40	6.8510×10^{-7}	9.5486×10^{-7}	2.87151×10^{-15}	4.55191×10^{-15}	1.77259	0.31250
80	1.7125×10^{-7}	2.3883×10^{-7}	1.28442×10^{-14}	1.81521×10^{-14}	1.99559	0.76563
100	1.0960×10^{-7}	1.5284×10^{-7}	1.64028×10^{-14}	2.28706×10^{-14}	2.11664	0.92188

6. Concluding Remarks

In conclusion, this paper presents a novel numerical technique for solving Burgers' equation using new cubic B-spline approximations. The proposed method offers several advantages over existing approaches, including improved accuracy and stability. Through a series of numerical experiments, we have demonstrated the reliability and efficiency of our scheme in capturing the behavior of Burgers' equation. The comparison between the approximate and exact solutions reveals the high accuracy achieved by our method, even with relatively coarse grid sizes. Moreover, the analysis of error norms confirms the superior performance of our approach compared to previous methods, showcasing its ability to yield highly accurate results. In summary, this paper presents a significant advancement in numerical techniques for solving Burgers' equation. The presented technique is more effective in comparison with the previous work of authors on various splines. The proposed method's high accuracy, stability, and convergence properties make it a promising tool for a wide range of applications in fluid dynamics and other related fields. Future research may focus on extending this approach to other partial differential equations and exploring its applicability in different physical scenarios.

Author Contributions: I.A., M.Y. and F.B.M.B.; methodology, M.A. and S.K.; software, M.Y., M.A. and S.K.; validation, I.A., M.Y. and F.B.M.B.; formal analysis, M.Y., M.A. and S.K.; investigation, I.A., M.Y., M.A., S.K. and F.B.M.B.; resources, I.A.; writing—original draft preparation, M.Y., M.A. and S.K.; writing—review and editing, I.A., M.Y., M.A., S.K. and F.B.M.B.; supervision, M.Y.; project administration, I.A., M.Y., M.A., S.K. and F.B.M.B.; funding acquisition, I.A. All authors have read and agreed to the published version of the manuscript.

Funding: This work was supported by the Deanship of Scientific Research, Vice Presidency for Graduate Studies and Scientific Research, King Faisal University, Saudi Arabia [GRANT No. 4011].

Data Availability Statement: Not applicable.

Acknowledgments: The authors extend their appreciation to the Deanship of Scientific Research, Vice Presidency for Graduate Studies and Scientific Research, King Faisal University, Saudi Arabia [GRANT No. 4011].

Conflicts of Interest: The authors declare no conflict of interest.

References

- Bateman, H. Some recent researches on the motion of fluids. *Mon. Weather. Rev.* **1915**, *43*, 163–170. [[CrossRef](#)]
- Fay, R.D. Plane sound waves of finite amplitude. *J. Acoust. Soc. Am.* **1931**, *3*, 222–241. [[CrossRef](#)]
- Burger, J.M. *A Mathematical Model Illustrating the Theory of Turbulence*, Advances in Applied Mechanics 1; Academic Press: New York, NY, USA, 1948; pp. 171–199.
- Cole, J.D. On a quasi-linear parabolic equations occurring in aerodynamics. *Q. Appl. Math.* **1951**, *9*, 225–236. [[CrossRef](#)]
- Hopf, E. The partial differential equation $U_t + UU_x = \mu U_{xx}$, *Commun. Pure Appl. Math.* **1950**, *3*, 201–230. [[CrossRef](#)]
- Kreiss, G.; Kreiss, H.O. Convergence to steady state solutions of Burgers' equation. *Appl. Numer. Math.* **1986**, *2*, 161–179. [[CrossRef](#)]
- Miller, E.L. Predictor–Corrector Studies of Burger's Model of Turbulent Flow. Master's Thesis, University of Delaware, Newark, DE, USA, 1966.
- Tian, Q.; Yang, X.; Zhang, X.; Xu, D. An implicit robust numerical scheme with graded meshes for the modified Burgers model with nonlocal dynamic properties. *Comput. Appl. Math.* **2023**, *42*, 26. [[CrossRef](#)]
- Jiang, X.; Wang, J.; Wang, W.; Zhang, H. A Predictor–Corrector Compact Difference Scheme for a Nonlinear Fractional Differential Equation. *Fractal Fract.* **2023**, *7*, 13. [[CrossRef](#)]
- Rodin, E.Y. On some approximate and exact solutions of boundary value problems for Burgers' equation. *J. Math. Anal. Appl.* **1970**, *30*, 401–414. [[CrossRef](#)]
- Benton, E.; Platzman, G.W. A table of solutions of the one-dimensional Burgers' equations. *Q. Appl. Math.* **1972**, *30*, 195–212. [[CrossRef](#)]
- Rubin, S.G.; Graves, R.A. *Cubic Spline Approximation for Problems in Fluid Mechanics*; National Aeronautics and Space Administration, TR R-436: Washington, DC, USA, 1975.
- Caldwell, J.; Wanless, P.; Cook, A.E. A finite element approach to Burgers' equation. *Appl. Math. Model.* **1981**, *5*, 189–193. [[CrossRef](#)]
- Caldwell, J.; Smith, P. Solution of Burger's equation with large Reynold's number. *Appl. Math. Model.* **1982**, *6*, 381–385. [[CrossRef](#)]
- Kadalbajoo, M.K.; Awasthi, A. A numerical method based on Crank–Nicolson scheme for Burgers' equation. *Appl. Math. Comput.* **2006**, *182*, 1430–1442. [[CrossRef](#)]

16. Rubin, S.G.; Khosla, P.K. Higher-order numerical solutions using cubic splines. *Am. Inst. Aeronaut. Astronaut.* **1976**, *14*, 851–858. [[CrossRef](#)]
17. Caldwell, J. Application of cubic splines to the nonlinear Burgers' equation. *Numer. Methods Nonlinear Probl.* **1987**, *3*, 253–261.
18. Nguyen, H.; Reynen, J. A space-time finite element approach to Burgers' equation. *Numer. Methods Nonlinear Probl.* **1987**, *3*, 718–728.
19. Jain, P.C.; Lohar, B.L. Cubic spline technique for coupled non-linear parabolic equations. *Comput. Math. Appl.* **1979**, *5*, 179–185. [[CrossRef](#)]
20. Lohar, B.L.; Jain, P.C. Variable mesh cubic spline technique for N-wave solution of Burgers' equation. *J. Comput. Phys.* **1981**, *39*, 433–442. [[CrossRef](#)]
21. Ali, A.H.A.; Gardner, L.R.T.; Gardner, G.A. *A Galerkin Approach to the Solution of Burgers' Equation*; University College of North Wales, School of Mathematics: Bangor, UK, 1990.
22. Ali, A.H.A.; Gardner, L.R.T.; Gardner, G.A. A collocation method for Burgers' equation using cubic splines. *Comput. Methods Appl. Mech. Eng.* **1992**, *100*, 325–337. [[CrossRef](#)]
23. Kutluay, S.; Bahadir, A.R.; Ozdes, A. Numerical solution of one-dimensional Burgers' equation: Explicit and exact-explicit finite difference methods. *J. Comput. Appl. Math.* **1999**, *103*, 251–261. [[CrossRef](#)]
24. Dağ, İ.; Irk, D.; Saka, B. A numerical solution of the Burgers' equation using cubic B-splines. *Appl. Math. Comput.* **2005**, *163*, 199–211.
25. Dağ, İ.; Irk, D.; Sahin, A. B-spline collocation methods for numerical solutions of the Burgers' equation. *Math. Probl. Eng.* **2005**, *5*, 521–538.
26. Abbasbandy, S.; Darvishi, M. A numerical solution of Burgers' equation by time discretization of Adomian's Decomposition Method. *Appl. Math. Comput.* **2005**, *170*, 95–102. [[CrossRef](#)]
27. Sarboland, M.; Aminataei, A. Taylor's meshless petrov–galerkin method for the numerical solution of Burgers' equation by radial basis functions. *Isrn Appl. Math.* **2012**, *15*, 254086.
28. Christie, I.; Griffiths, D.F.; Mitchell, A.R.; Sanz-Serna, J.M. Product approximation for non-linear problems in the finite element method. *Ima J. Numer. Anal.* **1981**, *1*, 253–266. [[CrossRef](#)]
29. Boor, C.D. On the convergence of odd degree spline interpolation. *J. Approx. Theory 1* **1968**, 452–463. [[CrossRef](#)]
30. Hall, C.A. On error bounds for spline interpolation. *J. Approx. Theory 1* **1968**, 209–218. [[CrossRef](#)]
31. Abdullah, M.; Yaseen, M.; de la Sen, M. Numerical simulation of the coupled viscous Burgers equation using the Hermite formula and cubic B-spline basis functions. *Phys. Scripta* **2020**, *95*, 115216. [[CrossRef](#)]
32. Yang, X.; Zhang, H. The uniform l1 long-time behavior of time discretization for time-fractional partial differential equations with nonsmooth data. *Appl. Math. Lett.* **2022**, *124*, 107644. [[CrossRef](#)]
33. Wei, L.; Yang, Y. Optimal order finite difference/local discontinuous Galerkin method for variable-order time-fractional diffusion equation. *J. Comput. Appl. Math.* **2021**, *383*, 113129.
34. Yang, X.; Wu, L.; Zhang, H. A space-time spectral order sinc-collocation method for the fourth-order nonlocal heat model arising in viscoelasticity. *Appl. Math. Comput.* **2023**, *457*, 128192.
35. Smaoui, N.; Belgacem, F. Connections between the convective diffusion and the forced Burgers Equation. *Appl. Math. Stoch. Anal.* **2002**, *15*, 53–69. [[CrossRef](#)]
36. Belgacem, F.; Smaoui, N. Interactions of parabolic convective diffusion equations and Navier-Stokes equations connected with population dispersal. *Commun. Appl. Nonlinear Anal.* **2001**, *8*, 47–67.
37. Herbst, B.M.; Schoombie, S.W.; Mitchell, A.R. A moving Petrov-Galerkin method for transport equations. *Int. J. Numer. Methods Eng.* **1982**, *18*, 1321–1336. [[CrossRef](#)]
38. Iqbal, M.K.; Abba, M.; Wasim, I. New cubic B-spline approximation for solving third order Emden-Flower type equations. *Appl. Math. Comput.* **2018**, *331*, 319–333. [[CrossRef](#)]
39. Yaseen, M.; Abbas, M. An efficient computational technique based on cubic trigonometric B-splines for time fractional Burgers' equation. *Int. J. Comput. Math.* **2020**, *97*, 725–738.

Disclaimer/Publisher's Note: The statements, opinions and data contained in all publications are solely those of the individual author(s) and contributor(s) and not of MDPI and/or the editor(s). MDPI and/or the editor(s) disclaim responsibility for any injury to people or property resulting from any ideas, methods, instructions or products referred to in the content.